Int J Earth Sci (Geol Rundsch) (2005) 94: 580–593
DOI 10.1007/s00531-005-0501-4

ORIGINAL PAPER

Ina Spottke · Eric Zechner · Peter Huggenberger

The southeastern border of the Upper Rhine Graben: a 3D geological model and its importance for tectonics and groundwater flow

Received: 23 October 2003 / Accepted: 28 March 2005 / Published online: 29 June 2005

Abstract A 3D geological model of the area east of Basel on the southeastern border of the Upper Rhine Graben, consisting of 47 faults and six stratigraphic horizons relevant for groundwater flow, was developed using borehole data, geological maps, geological cross sections, and outcrop data. This model provides new insight into the discussions about the kinematics of the area between the southeastern border of the Upper Rhine Graben and the Tabular Jura east of Basel. A 3D analysis showed that both thin-skinned and thick-skinned tectonic elements occur in the modeled area and that the Anticline and a series of narrow graben structures developed simultaneously during an extensional stress-field varying from E–W to SSE–NNW, which lasted from the Middle Eocene to Late Oligocene. In a new approach the faults and horizons of the 3D geological model were transferred into discrete elements with distributed hydrogeological properties in order to simulate the 3D groundwater flow regime within the modeled aquifers. A three-layer approach with a horizontal regularly spaced grid combined with an irregular property distribution of transmissivity in depth permitted the piezometric head of the steady-state model to be automatically calibrated to corresponding measurements using more than 200 piezometers. Groundwater modeling results demonstrated that large-scale industrial pumping affected the groundwater flow field in the Upper Muschelkalk aquifer at distances of up to 2 km to the south. The results of this research will act as the basis for further model developments, including salt dissolution and solute transport in the area, and may ultimately help to provide predictions for widespread land subsidence risks.

I. Spottke (✉) · E. Zechner · P. Huggenberger
Applied Geology Group, Department Geosciences,
University of Basel, Bernoullistrasse 32,
4056 Basel, Switzerland
E-mail: ina.spottke@unibas.ch
Tel.: +41-61-2673447
Fax: +41-61-2672998

Keywords 3D geological model · Groundwater flow model · Tabular Jura · Upper Rhine Graben

Introduction

Numerical simulation of groundwater flow has become a common hydrogeological tool to investigate a variety of geological settings. The reliability of these models largely depends on the capacity to predict the role of geological structures which control groundwater flow. Combined deterministic and stochastic techniques have been successfully applied to hydrogeological parameterization of unconsolidated sediments (e.g. Jussel et al. 1994; Regli et al. 2004). However, groundwater flow modeling in fissured and karstic aquifers is typically approached using deterministic methods for aquifer parameterization, especially in regional scale studies (e.g. D'Agnese et al. 1999; Kovacs 2003; Zechner and Frielinsdorf 2004). Geological discontinuities such as stratigraphic horizons and faults play a key role in controlling groundwater flow within fissured and karstic aquifers. Commonly used graphical user interfaces for groundwater simulation, such as GMS (2004), offer only limited possibilities for mapping geological settings with more complex tectonic structures. This is because (1) geological and geophysical data from different sources cannot be adequately imported and compared, (2) 3D structures such as faults and faulted stratigraphic horizons are very difficult to model accurately, (3) the consistency of a geological model of faulted horizons cannot be thoroughly reviewed, and (4) automated discretization of hydrogeological properties in such a setting is often not manageable by the graphical user interface.

This study investigated an 8 km by 8 km geologically complex area located at the southeastern border of the Upper Rhine Graben in the northwestern part of Switzerland to the east of Basel (Fig. 1). The area is underlain by Triassic and Jurassic strata that dip gently to the southeast and are subdivided by a series of NNE–SSW

striking horst and graben structures overlain by Quaternary sediments. A number of authors have proposed different tectonic models for the area implying different kinematic scenarios regarding the Southeastern Rhine Graben, most of which are based on incomplete data sets. The main differences between these models relates to the geometry and depth of the major fault zones and the relative age of the different tectonic structures. Most models explain only a part of the kinematic history by using 2D cross sections and focus on selected phenomena. None of the proposed models make use of 3D data or combine data to 3D objects such as stratigraphic horizons and faults.

The study site (Fig. 2) is part of an urbanized area that is currently experiencing large changes in industrial, commercial and transportation activities, including the recent construction of a tunnel for a more efficient north-south pan-European railway connection. Moreover, groundwater quality has been impacted by contamination that has occurred as a result of chemical spills and the deposition of hazardous waste. The Quaternary gravel aquifer is used for a regional drinking water supply in combination with an artificial groundwater recharge system, which was designed in order to maintain hydraulic gradients toward areas of potential risk. Apart from the public water supply system, large quantities of groundwater are abstracted for industrial purposes. Any potential change in this hydraulically complex system will result in impacts to groundwater quality and/or quantities for the existing users on the Swiss and also on the German part of the Rhine valley, immediately adjacent to this area. The regional groundwater system includes two main aquifers, the Quaternary Rhine gravel and the underlying karstified Triassic Upper Muschelkalk. The highly transient flow field is strongly influenced by the river groundwater interactions along the River Rhine, the structure of the complex aquifer-aquitard system and the groundwater production for water supply and industry. Knowledge of the connectivity between surficial and deeper aquifers is fundamental for understanding the regional and local scale groundwater flow pattern in this area.

In this study we present a new approach of integrating geological data into a hydrogeological model. Firstly, in order to integrate as much of the existing geologic information as possible, we constructed a 3D geological model of the area, which is based on the existing geological information (borehole descriptions, geological maps, geological cross-sections) that is consistent with the regional geological setting. The geological 3D model was constructed using a software package capable of modeling complex geological objects (GOCAD; Geological Objects Computer Aided Design). The model includes 47 faults and four faulted horizons in order to derive structural maps of the main aquifers-aquitards boundaries. Secondly, we integrated the faulted horizons of the 3D geological model into the groundwater modeling software package GMS (2004) and simulated the groundwater flow within the main relevant aquifers using a finite difference approach.

The results of the research presented herein form a base for further model development, which will help to focus on the causes of the subsurface salt dissolution, and ultimately provide predictions on land subsidence risks in the area. In addition, the regional scale groundwater model can be used as a decision tool for sustainable groundwater management in the Muttenz-Pratteln area (Fig. 2). The 3D geological model presented herein also acts as an excellent platform for evaluating the impact of future infrastructural developments and will be applicable for any 3D data queries regarding different aspects of the geology of the area.

Geological setting

The Muttenz-Pratteln area (Fig. 2) is situated to the east of the southeastern border of the Upper Rhine Graben within the Dinkelberg Block. This block forms part of the Tabular Jura and is influenced by the Rhine-Bresse Transfer Zone (Fig. 1). The Rhine-Bresse Transfer Zone strikes E–W, has a complex composition and diffuse borders. The fracture zone is 40 km wide and partially transfers the dilation from the Rhine graben into the Bresse graben (Laubscher 1971).

The Dinkelberg Block is bounded by the Rhine Valley Flexure, the Kandern Fault, the Werratal Fault and the Zeiningen Fault (Fig. 2). The block boundary is poorly defined to the south. Within the block, the Maulburg and Rheinfelden Faults act as boundaries to the Dinkelberg Graben. The entire Dinkelberg Block is characterized by a set of NNE–SSW striking narrow graben structures that have unknown shape and depth. In the southern part of the Dinkelberg Block, the

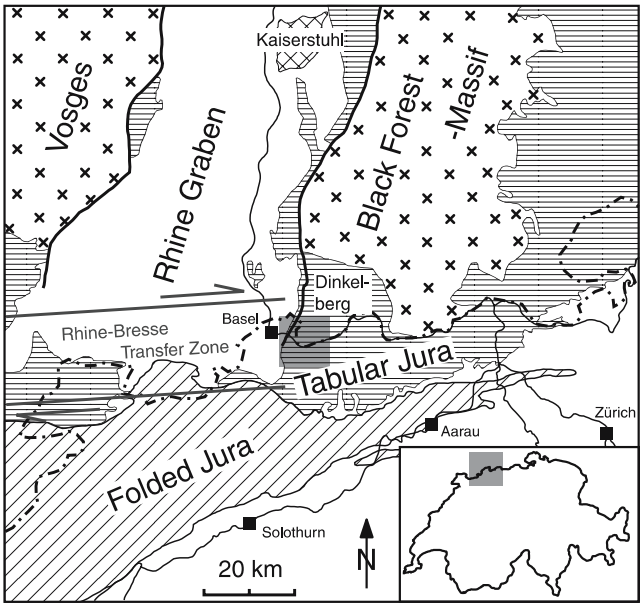

Fig. 1 Regional overview with working area (modified after Thury et al. 1994)

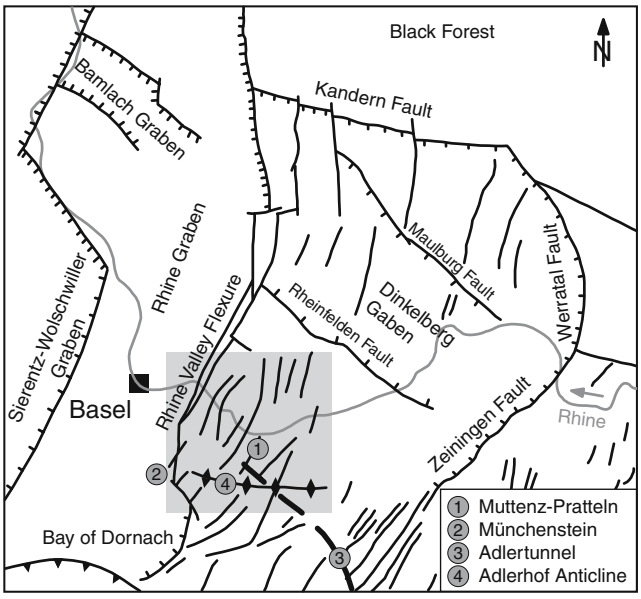

Fig. 2 Tectonic overview (*grey square* = working area)

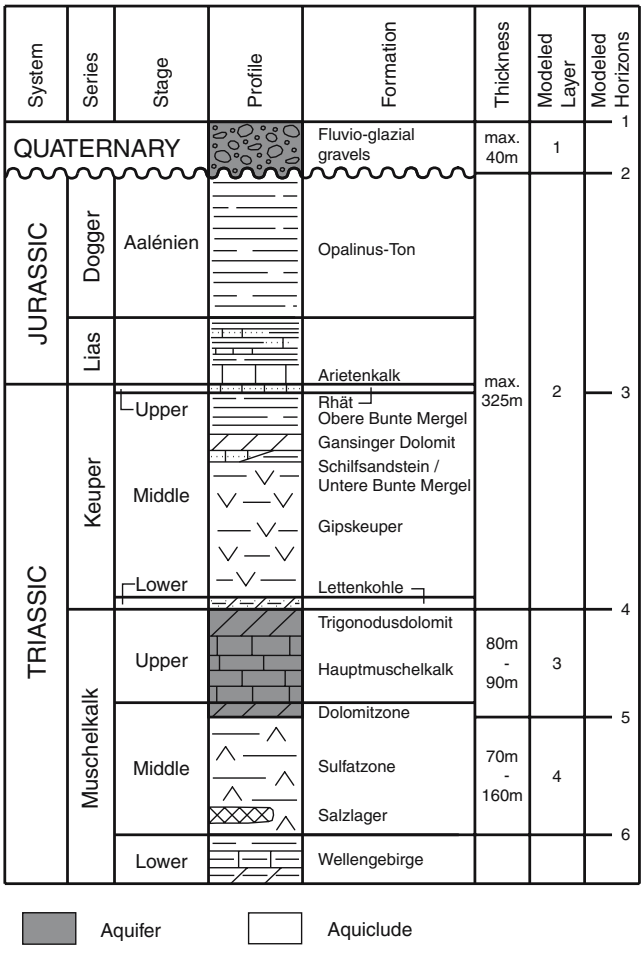

Fig. 3 Lithostratigraphy, hydrostratigraphy and modeled horizons (modified after Bitterli-Brunner et al. 1988; Gürler et al. 1987 and Pearson et al. 1991)

ESE–WNW striking Adlerhof Anticline represents a compressive structure.

The area under study is underlain by Triassic and Jurassic strata, which dip slightly to the southeast. Herzog (1956) provided the first comprehensive description of these strata (Bitterli-Brunner et al. 1984), including an annex (Bitterli-Brunner et al. 1989), with a stratigraphic column that acted as the basis for Fig. 3.

The stratigraphic column extends from the Quaternary to the the Lower Muschelkalk. This sequence is relevant for the geological and hydrogeological modeling. The lowest lithostratigraphic unit in the area studied is the Lower Muschelkalk, which consists of a succession of marine dolomites, calcareous mudstones, and bituminous dolomitic mudstones approximately 40 m thick. The overlying Middle Muschelkalk, is subdivided into the *Sulfatzone* and the *Dolomitzone*, respectively. The *Sulfatzone* is made up of dolomitic marls, anhydrite and gypsum, with intercalations of clay and marl and varies in thickness from 30 to 130 m. A salt layer (*Salzlager*), up to 50 m thick occurs in the lower part. The *Dolomitzone* consists of a 10 m thick sequence of porous dolomite. The lower part of the Upper Muschelkalk consists of a 50–60 m thick series of limestones (*Hauptmuschelkalk*). The upper part consists of approximately 20 m of *Trigonodusdolomit*. The overlaying Keuper unit has a thickness of 130 –170 m. The *Lettenkohle* (about 5 m) at the base and the *Rhät* (about 5 m) at the top of the Keuper reflect the continental influence on sedimentation during the time that this unit was deposited. The 60–100 m thick *Gipskeuper* overlying the *Lettenkohle* consists of marls with gypsum and anhydrite lenses. The following sandstones and marls of the *Schilfsandstein*/*Untere Bunte Mergel* reflect a complex pattern of facies changes and have a thickness of 20–25 m. The *Gansinger Dolomit* (about 10 m) consists of shallow marine dolomite. It is followed by a 30 m thick sequence of greyish to reddish marls and clays (*Obere Bunte Mergel*). During the Lias, marls and shales were deposited in a shallow marine environment (20–40 m thick). Embedded into these sediments is a 5 m thick, fossil rich, competent, porous limestone (*Arietenkalk*). The uppermost 80–100 m of the occurring Mesozoic unit consists of a dark grey silty micaeous clay (*Opalinuston*).

These Triassic and Jurassic strata are separated from a Quaternary cover by an unconformity. The Quaternary cover consists of fluvio-glacial gravels that are up to 40 m thick. This unit represents an accumulation of different types of gravel sheets. Several depositional terraces, separated from each other by terrace bluffs, exist in the area.

Triassic and Jurassic strata were deformed by the Rhine Valley Flexure, the Adlerhof Fold and narrow graben structures. Herzog (1956) explained the development of these structures by the following sequence of events: (1) the Adlerhof Anticline was formed before the Rhine Valley Flexure, (2) the Adlerhof Anticline developed before the NNE–SSW striking faults in the Tabular

Jura, (3) the Adlerhof Anticline has been folded in several steps, of which the last probably developed after the genesis of faults, (4) a pre-Miocene age can be assumed for the NNE–SSW striking faults, (5) there is no evidence for younger movements (Miocene to Quaternary). Laubscher (1982) interpreted the horst and graben structures of the Tabular Jura in the Muttenz-Pratteln area and the Adlerhof Anticline as the combination of (a) the detachment of the sedimentary cover from the crystalline basement to the north by gravity gliding and (b) the development of the Rhine valley flexure towards the west. The idea of detachment of the sedimentary cover (thin-skinned model) contrasts with the subvertical fault interpretation proposed by Gürler et al. (1987). These faults appear to originate at the basement and continue through its sedimentary cover indicating that a combination of thick-skinned and thin-skinned kinematics was active during the Tertiary. Schmassmann (1990) proposed that the master faults of the graben structure converge with depth and generally terminate in Middle Triassic deposits, except for larger faults, which can reach the Lower Triassic and the crystalline basement. The geological profile constructed by Meyer (2001) along the Adlertunnel axis, incorporates the new geological observations and drill-core data from the tunnels construction (Figs. 2, 5). The principal importance of this work relates to the presentation of south verging thrusts within the Adlerhof Anticline. Laubscher (2003) considers the Aspenrain Fault and the Adlerhof Fold as a composite structure (“Adlerhof Structure”) that has developed since the Early Miocene by limited detachment in the Middle Triassic (Herzog 1956; Hauber 1971; Gürler et al. 1987) under dextral transpression along a SE–NW oriented σ_1 axis. Laubscher (2001, 2003) proposed a forerunner of the Adlerhof Structure of Eocene age to explain the discontinuity of the NNE–SSW striking graben structures across the Adlerhof Fold (Bitterli-Brunner et al. 1984) together with an Eocene age for most of the Tabular Jura grabens.

To conclude, the development of the Rhine Valley Flexure, the Adlerhof Fold and the narrow graben structures have been interpreted by the different authors as a consequence of either thin-skinned or thick-skinned tectonics.

Hydrogeological setting

There have been few regional scale studies showing the close relationship between groundwater flow and tectonic setting in this area. Schmassmann (1990) provides the most recent and extensive study of this subject. This work presented a qualitative characterization of both the Quaternary and the Upper Muschelkalk Aquifers and recognized the importance of the graben structures for groundwater flow by collecting hydrochemical data and constructing geological maps and geological profiles based on existing drill-core data. The only numerical groundwater model of the area prior to the current study has been developed by Trösch et al. (1997). The aim of this transient model study was to simulate the joint effects of artificial groundwater recharge and potable groundwater pumping in the Hardwald area. Hardwald is located in the northwestern part of the study area between Rhine Valley Flexure and Hard Graben (Fig. 5). Recharge occurs in this area by discharging surface water from the Rhine into smaller artificial rivers and ponds. The 2D Finite Element approach chosen by Trösch et al. (1997) required a vertical averaging of the hydrogeological properties over all relevant aquifers and aquitards. The authors observed larger discrepancies between hydraulic head measurements and corresponding model results along the Rhine Valley Flexure and the bordering faults of the Hard Graben. They attributed these discrepancies to the limited capacity of a 2D groundwater model to simulate groundwater flow in the geological setting presented herein.

We grouped lithostratigraphic units into four main hydrostratigraphic layers according to their hydraulic properties (Fig. 3). The Lower Muschelkalk and the evaporites of the Middle Muschelkalk are widely considered as impermeable throughout Northern and Northwestern Switzerland (Nagra 1988, 2002; Gürler et al. 1987). They form a lower aquiclude (layer 4), which serves as confining unit for the overlying aquifer. However, within the Middle Muschelkalk a gypsum karst unit, approximately 10 m thick, has been observed between the top of the salt layer and the anhydrite of the Upper Sulfate Zone (Aegerter and Bosshardt 1999). The amount of groundwater stored in this unit is negligible on a regional scale (Gürler et al. 1987), but the aquifer probably transports groundwater that leaches the underlying halite. The Dolomite Zone of the Middle Muschelkalk, and the Upper Muschelkalk, form the lower aquifer (layer 3). Both units are highly porous, fractured and karstified. They represent an important aquifer at the local and regional scale (Nagra 1988, 2002; Gürler et al. 1987; Schmassmann 1990). Saladin (unpublished data) determined an average hydraulic conductivity of 1.3×10^{-4} m/s in hydraulic tests conducted in boreholes of the Upper Muschelkalk Aquifer within the study area. This hydraulic conductivity and unit thicknesses of 50–80 m results in transmissivities of up to 1×10^{-1} m^2/s, thus making the unit a regionally important aquifer. The overlaying sediments of Keuper, Lias and Lower Dogger mainly consist of marls and clays and were defined as the upper aquiclude (layer 2), due to their low to very low permeabilities. Hydraulic conductivities for these sediments as tested in borehole and modeling studies in Northern Switzerland (Nagra 2002) were between 1×10^{-14} and 1×10^{-7} m/s. Small aquifers were found in sandstone and dolomite beds of the Keuper, but according to Gürler et al. (1987), their importance can be neglected compared to that of the Upper Muschelkalk Aquifer. The upper aquifer of the study site is located in the Quaternary Rhine gravels (layer 1). Typical saturated thicknesses range between 10 m and 20 m, but may reach more than 30 m in certain parts. Hydraulic conductivities

determined from 56 pumping tests in the study area had an average value of 3.1×10^{-3} m/s for the Quaternary Aquifer (Saladin, unpublished data). Other aquifers of regional importance are the Buntsandstein/Perm/Crystaline Basement and the Oxfordian carbonates. These units, however, are not relevant for the present study as they are either hydraulically unconnected (Buntsandstein/Perm/Crystaline Basement), or have been eroded (Oxfordian carbonates). In summary, there are two aquifers; the mainly confined karstic Upper Muschelkalk Aquifer (layer 3), and the unconfined Quaternary Gravel Aquifer (layer 1).

Fracture zones causing increased permeability within the formations may favor vertical exchange of groundwater also across aquitards. Gürler et al. (1987) pointed out, that intensively faulted and fractured zones mostly simplify water circulation, which according to Hauber (1971), leads to a gradual natural solution of the Salzlager. Consequently, modeling vertical transport of dissolved salt requires increased hydraulic conductivities along fault zones since the aquitard of the Upper Sulphate Zone in between the salt formation and the Upper Muschelkalk Aquifer restricts vertical fluxes. In the present modeling study, however, transport of dissolved salt is not simulated. At the regional scale (several km), the connectivity of aquifers and aquicludes is primarily influenced by the tectonic setting of horst and graben structures. The general dip of the Mesozoic strata to the SE results in a direct contact between the Quaternary Aquifer and the Upper Muschelkalk Aquifer, mainly in the northwestern parts of the model area. The graben structures produce different connectivity scenarios: they either completely or partly penetrate the aquifer, depending on the offset along the bounding normal faults.

The general flow direction of the Rhine River in the Tabular Jura is from east to west. Filtration along the River Rhine is proportional to the difference between river level and hydraulic head in the connected aquifer. The river level, however, does not vary significantly upstream of the ''Birsfelden'' log, which is located 1.5 km downstream of the Rhine Valley Flexure. Consequently, the exchanging fluxes mostly depend on the transient hydraulic groundwater head. Large-scale groundwater pumping for industrial use results in increased infiltration in the sections of the Rhine located in the central part of the study area around the Wartenberg Graben (Fig. 5). All other sections are exfiltrating, with increased exfiltration due to the artificial recharge along the Hardwald area in the northwestern part of the model.

3D Geological model

Data sources

The first step in building a 3D model involved data collection. The more consistent the available data the better the resulting model will be. In the current case, input data of different type and quality were available. Due to varying data origins, incompatibilities occurred between the different types of data.

- A digital elevation model employing a 25 m grid interval as base for a topographic surface (DHM25, The Federal Office of Topography, Wabern) was used.
- Borehole data were employed to reconstruct geological surfaces. Approximately 8,200 borehole data of differing depths were compiled in the GEODATA database (Noack 1993) of the Applied Geology Group at the University of Basel. GEODATA contains export possibilities for different file formats, which allow the user to export self-defined data sets. Consequently, it was possible to export the *x*-, *y*-, *z*-coordinates for every layer boundary of interest: 750 boreholes end slightly below the pre-Quaternary surface, and 128 boreholes reach a depth of 100–400 m (Fig. 7A).
- The other fundamental data source for the construction of geological surfaces are existing geological maps (Bitterli-Brunner et al. 1984; Wittmann et al. 1970) and cross sections (Herzog 1956; Gürler et al. 1987; Bitterli-Brunner et al. 1989; Schmassmann 1990; Meyer 2001). Layer boundaries and fault traces were digitized with a customized software routine, which also included export possibilities for different file formats. The cross sections used differ in scale, fault position and fault geometry as a result of different geological interpretations. Gürler et al. (1987) and Meyer (2001) used straight fault geometries as their interpretations correspond to thick-skinned tectonics, whereas Herzog (1956), Bitterli-Brunner et al. (1989) and Schmassmann (1990) used listric fault geometries representing thin-skinned tectonics.
- Outcrop data was also incorporated. The dips of stratigraphic layers were measured and fault positions mapped. The outcrop information focuses on the southern part of the area of interest and represents a small but very important part of input data for the geological model.
- Finally, the results of a geoelectrical survey were employed. In this research campaign, we worked with an earth resistivity meter and a multi-electrode cable for surface-based measurements of cross sections in order to estimate formation thicknesses and fault positions (Spottke, unpublished data).

Methodology

The geomodeling method employed in this study was defined by Mallet (2002) as follows: ''Geomodeling consists of the set of all mathematical methods allowing modeling the topology, the geometry and the physical properties of geological objects in a unified way while taking into account any type of data related to these objects.''

GOCAD, which was used in this study, is one of the leading software packages employed in geomodeling.

GOCAD allows the user to construct, visualize and edit topographical and geological data in different object classes (e.g. points, lines, surfaces, volumes, wells). The modeling engine for this software is based on the interpolation algorithm Discrete Smooth Interpolator (DSI) (Mallet 1989, 1992, 2002). This interpolation algorithm respects soft and hard constraints in order to fix points, lines, surfaces, regions or properties at specific *x*-, *y*-, *z*-coordinates.

The modeling was subdivided into different steps. The first step consisted of importing data into the modeling software (Fig. 4A). The second step involved the construction of faults and horizons (Fig. 4B). The fault planes were constrained using fault lines on geological maps, fault traces on geological cross sections and fault markers in well data. The contacts between fault planes were defined. This definition determined how fault planes were cut with each other. By respecting the defined geometry and the defined contacts, the interpolation algorithm was applied. The horizons were constrained by well data, geological maps, geological cross sections and outcrops. Furthermore, the constructed horizons were cut with the fault system. This required the definition of contacts between horizons and fault plans by setting constraints on horizon boundaries. The interpolation algorithm was run while respecting the defined geometry and the defined contacts. Finally the resulting fault-horizon-model (Fig. 4C) was thoroughly verified by exporting geological cross sections from the 3D model.

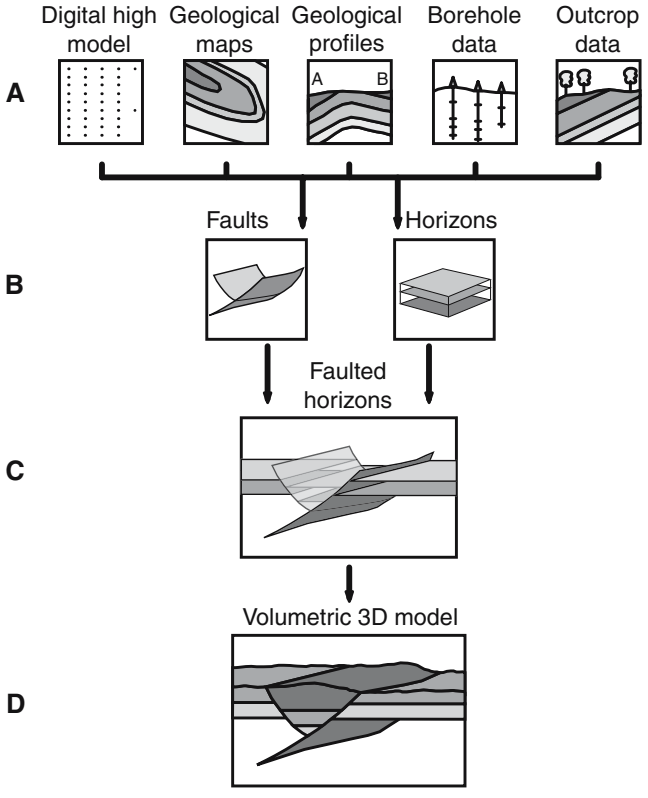

Fig. 4 Schematic modeling procedure, **A** input data, **B** modeling of surfaces, **C** modeling of faulted horizons, **D** construction of the volumetric 3D model)

In order to model faults and horizons, it was necessary to make three assumptions. The first assumption related to complex tectonic elements. In order to keep the amount of data manageable, a simplification was necessary for the modeling. This meant that a fault zone was modeled as a single fault plane. Consequently, graben structures are simplified in the model. Secondly, we assumed that the pre-Quaternary surface was equal to the topography in the hilly parts of the model. This assumption is acceptable as Quaternary deposits are either less important or absent in these areas. The third assumption related to the decision on how many horizons should be modeled. We defined the number of horizons by the number of main aquifer–aquiclude boundaries (Fig. 3). Two exceptions were made: (a) where the base of the Lower Muschelkalk represents the lower boundary of the lower aquiclude, the top of the Lower Muschelkalk was modeled, due to the absence of raw data for the base of the Lower Muschelkalk, (b) in order to visualize the sediment filling of graben structures, the top of the Keuper (Rhät) was also modeled, although it does not represent an aquifer–aquiclude boundary.

Results

Geomodeling provided a 3D geological model, which is bounded by the Grenzach-Wyhlen Fault, the eastern border of the Rhine Valley Flexure, the Aspenrain Fault and the eastern border of the Adler Graben System (Fig. 5). Within the model, the following tectonic subunits occur: the Hard Graben System, the Wartenberg Graben System, the Cholholz Graben System, the Cholholz Fault, the Adler Graben System and the Adlerhof Anticline (Figs. 5, 6). The model extends vertically from the surface to the top of the Lower Muschelkalk. In addition to the surface topography, we modeled the pre-Quaternary surface and the following four faulted horizons: the top of the Keuper, the top of the Upper Muschelkalk, the top of the Sulfatzone, and the top of the Lower Muschelkalk (Figs. 6, 7).

Faults

The fault system in the modeled area consisted of five different elements: (a) the Rhine Valley Flexure, (b) the Grenzach-Wyhlen Fault, (c) the Aspenrain Fault, and (d) the narrow graben structures. A total of 47 faults were modeled (Fig. 5).

In the model the Rhine Valley Flexure was simplified to two planar, approximately parallel faults. These faults strike NNE–SSW (Fig. 5), dip at 75° to WNW (Fig. 6A, B), and mark the borders of the flexure zone. The eastern fault also acts as the western border of the geological model (Fig. 5).

The Grenzach-Wyhlen Fault has an orientation of ESE–WNW and dips with 70° to the SSW. The planar

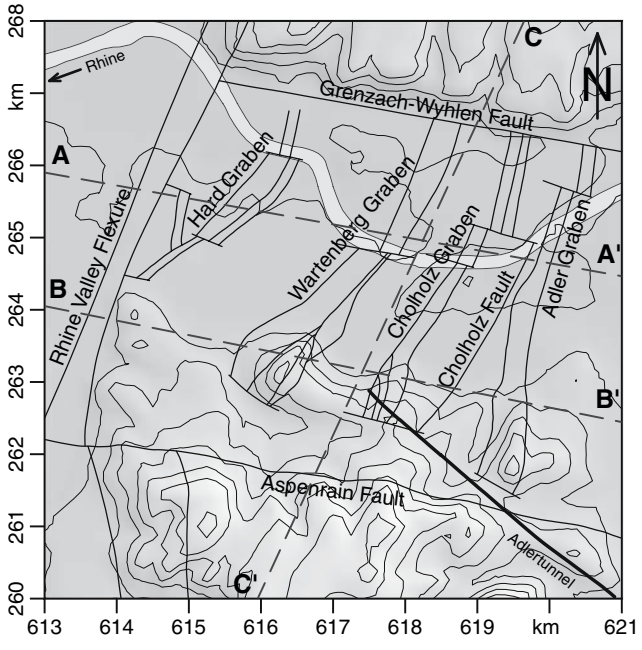

Fig. 5 Fault system on Pre-Quaternary surface (A–A′, B–B′ and C–C′ = cross sections (see Fig. 6))

normal fault indicates a displacement of about 80 m in the Lower Muschelkalk Horizon (Figs. 5, 6C, 7F). The Grenzach-Wyhlen Fault represents the northern border of the model.

The Aspenrain Fault defines the southern border of the model (Fig. 5). This fault strikes ESE–WNW and dips to the south, extending from the crystalline basement to the top of the Lower Muschelkalk, with a dip of 70°. Closer to the surface the dip declines gradually to 50° (Fig. 6C). Displacement amounts to approximately 150 m. Near Münchenstein, the Aspenrain Fault is in contact with the Rhine Valley Flexure (Figs. 2, 5). The Rhine Valley Flexure, the Grenzach-Wyhlen Fault and the Aspenrain Fault end in the crystalline basement, suggesting thick-skinned tectonics features.

The narrow graben structures are oriented NNE–SSW. From west to east four graben systems occur, which have been named Hard Graben, Wartenberg Graben, Cholholz Graben (including the Cholholz Fault), and Adler Graben (Figs. 5, 6A, B). These graben systems are subdivided by tear faults. Initially these tear faults were not traced as there was no information about their occurrence. However, the digitized fault traces and lines together with the borehole information required faults to have an abnormal s-shaped curvature; this could only be prevented by dividing the narrow graben structures with tear faults (Fig. 5). All tear faults are vertical. The graben faults and tear faults end in the Sulfatzone. The structure of the top of the Upper Muschelkalk Horizon, in which no evidence for graben structures could be found, suggests the faults terminate in the Sulfatzone. Consequently, the graben faults are modeled as listric features (thin-skinned tectonics). In each graben system, the eastern fault is the master fault of the graben system, which means that the principal displacements occur along the eastern graben faults (Fig. 6A, B). The displacements determined on each of the eastern master faults were as follows: Wartenberg Graben, about 200 m at the top of the Keuper Horizon; Cholholz Graben, about 80 m at the top of the Upper Muschelkalk Horizon; Cholholz Fault, approximately 100 m at the top of the Sulfatzone Horizon and Adler Graben, about 70 m at the top of the Upper Muschelkalk Horizon (Fig. 6B). The amount of displacement in

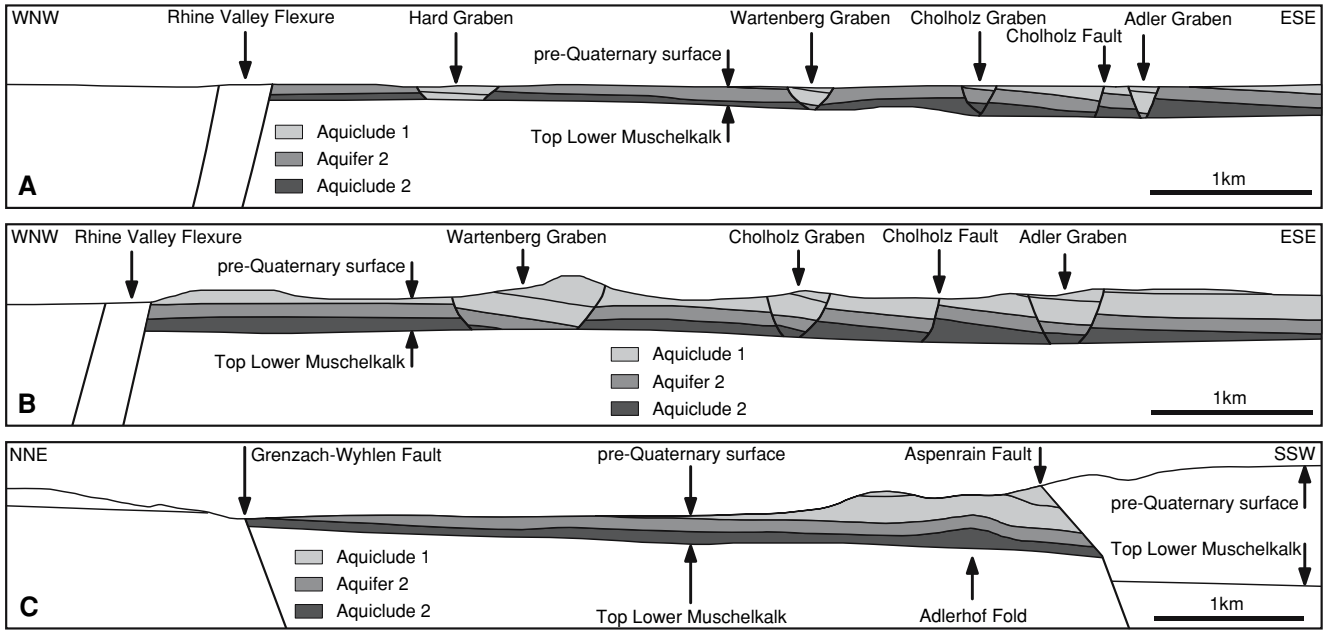

Fig. 6 Cross sections across the modeled area (cross-section traces see Fig. 5)

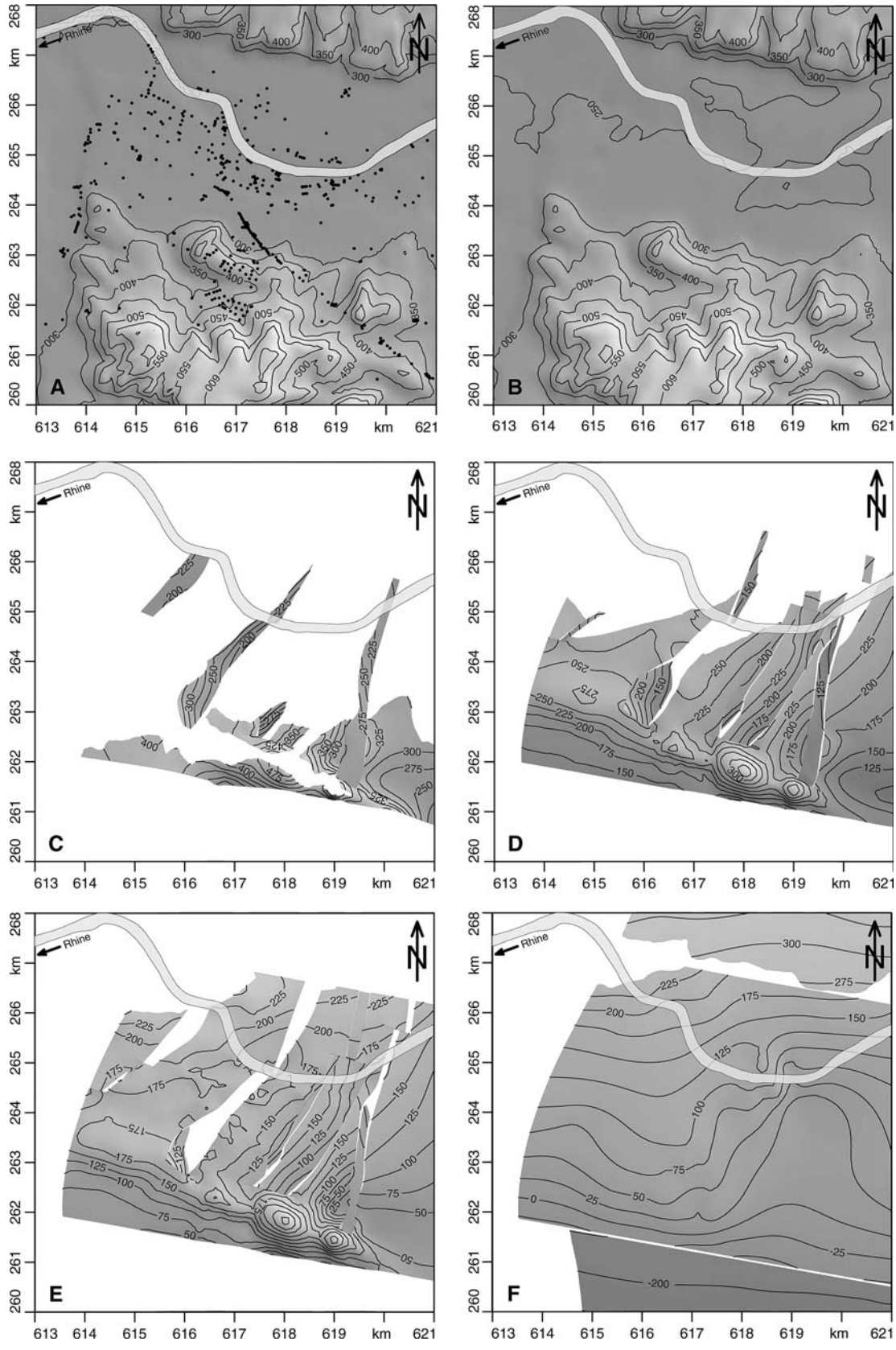

Fig. 7 Modeled horizons, **a** topography, **b** pre-Quaternary surface, **c** Top Keuper, **d** Top Upper Muschelkalk, **E** Top Sulfatzone, **F** Top lower Muschelkalk). *Black points* in **A** represent the distribution of borehole data

the Hard Graben is about 200 m and is documented by the existence of the top of the Keuper Horizon inside the graben adjacent to the top of the Sulfatzone Horizon outside the graben (Fig. 6A).

Horizons

The 3D model incorporates the six horizons that are most influential for groundwater flow (see Fig. 3), namely: (1) topography, (2) pre-Quaternary surface, (3) top of the Keuper, (4) top of the Upper Muschelkalk, (5) top of the Sulfatzone, and (6) top of the Lower Muschelkalk. These surfaces correspond to the main aquifer–aquiclude boundaries (see section Hydrogeological setting).

The topography model shows higher elevations to the north and south of the Rhine Valley, which is oriented east–west (Fig. 7A). The maximum elevation of 663 m above sea level is located at 617.628, 260.876 (Swiss national topographic grid (SNTG)). The minimum elevation at the bottom of the Rhine is 246 m above sea level at 615.730, 266.530 (SNTG). The pre-Quaternary surface is similar to the present day topography (Fig. 8B). Differences only appear in the Rhine Valley, where Quaternary alluvial deposits cover the bedrock. The minimum elevation of the pre-Quaternary surface of 223 m above sea level is located at 615.250, 266.125 (SNTG). The topographic surface and the pre-Quaternary surface occurs at the margins of the uppermost aquifer, the Quaternary gravels. The thickness of this layer varies between 0 m and 48 m.

The faulted horizon model dips at a low angle to the southeast and cut the pre-Quaternary surface (Figs. 5, 6, 7) resulting in an erosional discontinuity.

The Keuper Horizon occurs inside the graben structures and in the southern part of the model (Fig. 7C). The horizon appears in the middle part of the Hard Graben, in the Wartenberg Graben, in the southern parts of the Cholholz Graben and the Adler Graben (Fig. 6A, B; black line inside aquiclude 1). Along the crest line of the Adlerhof Fold, the top of the Keuper Horizon is eroded (Fig. 7C).

The top of the Sulfatzone and the top of the Upper Muschelkalk occur below the Keuper, (Fig. 7D, E). These horizons clearly display the structure of the Adlerhof Anticline south of the graben structures and north of the Aspenrain Fault. The Adlerhof Anticline strikes ESE–WNW, but its orientation is not parallel to the Aspenrain Fault. From west to east both structures almost converge towards the southeast corner of the model. At this location the anticline has a gently sloping northern limb and a steeply sloping southern limb (Fig. 6C). Farther west, the fold is wider and the limbs become more symmetrical. The Adlerhof Anticline consists of a number of ESE–WNW striking parts, which are arranged in an en-échelon configuration.

In contrast, the top of the Lower Muschelkalk is influenced neither by the graben structures nor the Adlerhof Anticline. The horizon has an elevation of 225 m above sea level in the NW, and an elevation of 50 m below sea level in the SE (Fig. 7F). The Lower Muschelkalk Horizon is displaced by 80 m to the north by the Grenzach-Wyhlen Fault and by 150 m to the south by the Aspenrain Fault (Fig. 6C).

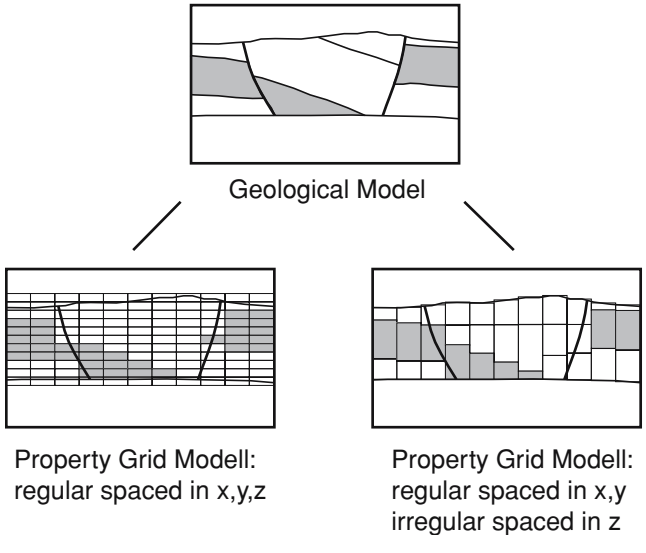

Fig. 8 Schematic grid discretization for 3D numerical groundwater (karst aquifer is in *grey color*; aquicludes/aquitards are in *white color*)

3D groundwater flow model

Groundwater flow within the study area is strongly influenced by the geometry and thickness of the Quaternary alluvial deposits, the geological structure of the NNE–SSW trending horsts and grabens, and the hydraulic boundary conditions, such as river level in the Rhine, or groundwater pumping and artificial recharge. The numerical simulation of groundwater flow requires an appropriate transfer of the 3D horizons and faults into discrete elements with distributed hydraulic conductivity and storage capacity. An additional problem arises in the simulation of groundwater in karst systems. This is due to the difficulty in developing numerical models that realistically represent double-continuum media (conduit network and matrix) typical for karstic aquifers (Kovacs 2003). The single-continuum approach used for groundwater flow in porous aquifers is appropriate for the flow simulation in carbonate aquifers of regional scale with comparable small solution cavities and an absence of a well-developed conduit network (Zechner and Frielinsdorf 2004).

Methodology

In order to simulate groundwater flow, the 3D finite difference code MODFLOW (Harbaugh et al. 2000) was employed in combination with the graphical user interface GMS v4.0 (2004). The advantages of MODFLOW

include the versatility of its modular concept, the robustness of the method for groundwater flow simulation in formations with highly varying hydraulic conductivities, and the abundance of pre- and postprocessing software. The main disadvantage of using this approach is that the regularly structured model grid cannot directly represent 3D geometries. GOCAD does not provide any routine to export hydrogeologic property grids which could be directly input into MODFLOW. Consequently, two methods of translating 3D faults and horizons were compared, namely (Fig. 8) (1) conversion of the geological fault horizons into a volumetric model of regularly spaced cells inside GOCAD, with properties directly assigned to the cells; and exporting the property grid with subsequent transformation into the corresponding MODFLOW package; (2) transfer of the faulted horizons model from GOCAD into the pre-processor GMS using the Triangular Irregular Network format (TIN).

The first method required a grid resolution of 50 m(x) by 50 m(y) by 25 m(z) per cell. This is a compromise between an adequate representation of the geology and a manageable grid size of 1,024,000 cells covering the study area. Property assignment was done by a simple decision: cells crossing a fault or a horizon belong to the hydrostratigaphic formation where most of the cell volume is located. Properties are located in the center of the cell. The advantage of this method is that subvertical structures such as grabens are more accurately represented with a 25-layer grid. A major disadvantage of this approach, however, is the sudden jumps in size of 25 m in the discretization of subhorizontal horizons, which lead to inconsistencies mainly in the 10–30 m thick Quaternary Aquifer at the top of the model. The large grid size also requires excessive computational time when simulating groundwater flow by iterative methods for automated estimation of aquifer properties.

As a consequence of the above constraints, we employed a second method that exported the faulted horizons from GOCAD (Fig. 8B) by modifying the data file in order to allow GMS to read the data in a TIN format. The TIN nodes were used to interpolate the structures of the two main aquifers and the intermediate aquitard to a 3-layer model. The *top* model layer represents the unconfined Quaternary Alluvial Aquifer, which is bound on the bottom by the pre-Quaternary surface and on top by the simulated piezometric head. The *intermediate* layer has a dual function. In the southeast of the model domain, it represents the Keuper aquiclude with the bounding pre-Quaternary surface on top, and the top of the Upper Muschelkalk at the bottom, thereby restricting groundwater exchange between the two aquifers. In the northwestern part, where the Keuper is eroded, the *intermediate* layer is modeled as being a few meters thick and adopts the properties of the Upper Muschelkalk Aquifer in order to model the unrestricted exchange between the two aquifers. The *bottom* model layer represents the Upper Muschelkalk Aquifer with the top of the Sulfatzone at the bottom. The horizontal discretization of the grid is regular (50 by 50 m), but MODFLOW permits transmissivity (hydraulic conductivity multiplied by vertical layer thickness) to be varied continuously within each layer. Consequently, we obtain an accurate representation of the thickness variations of the modeled formations. Existing graben structures, however, were approximated in the model. If the offset of the graben bordering fault was thicker than the Muschelkalk Aquifer, then they were modeled as vertical model blocks through both *intermediate* and *bottom* layers, and, thus, restricting groundwater flux below the graben. If its offset is significantly less important than the thickness of the Muschelkalk Aquifer, then the graben block is only modeled as an *intermediate* layer.

Data sources

Initial model values of the hydraulic conductivities (K) for the two aquifers are based on the averaged analyses of the results of hydraulic borehole tests presented by Saladin (Saladin, unpublished data). The values are 3.1×10^{-3} m/s for the Quaternary Aquifer and 1.3×10^{-4} m/s for the Upper Muschelkalk Aquifer. Hydraulic boundary conditions of the simulation were defined using averaged pumping rate data, river stage and measured hydraulic heads on outer boundaries from 1st to 8th of August, 2003. During this period, overall groundwater pumping rates were 2.2 m^3/s, and artificial recharge reached more than 1.0 m^3/s in the western part of the Quaternary Aquifer (Hardwald). Outer boundaries were defined with prescribed heads at both the eastern and western ends of the model layer 1, which corresponds to the Quaternary Aquifer. All other outer boundaries through all three layers were set as no-flow boundaries. The River Rhine was simulated employing a mixed-type boundary condition, where infiltration and exfiltration are calculated in proportion to the differences between river level and hydraulic groundwater head, and an initial leakage factor of 2.5×10^{-6} s^{-1}. This factor was subsequently adjusted during the model calibration. The simulated piezometric head of the steady-state model was calibrated to corresponding measurements taken in more than 200 piezometers on August 8th, 2003.

Results

The initial hydraulic properties were determined by employing the automated parameter estimation procedure within the nonlinear regression code UCODE (Poeter and Hill 1998). Optimal parameters resulted in hydraulic conductivities of 4.7×10^{-3} m/s for the Quaternary Aquifer, 7.4×10^{-4} m/s for the Muschelkalk Aquifer, and 8.1×10^{-6} m/s for the confining Keuper aquitard. The simulated distribution of hydraulic head in both major aquifer layers shows the influence of

artificial recharge in the northwestern model part (Fig. 9). The large-scale industrial pumping rate of up to 1500 l/s in the central part of the model area results in three important cones of depression up to 2 km wide in the Upper Muschelkalk Aquifer. No significant hydraulic gradient is observed in the southern part of the model, which corresponds to the position of the Adlerhof Anticline. General groundwater flow velocities along the southern model boundaries are thus relatively slow. But the flow pattern along the Adlerhof Anticline is also influenced by the industrial pumping and is directed around the Southern ends of the Graben structures, i.e. groundwater flows around the Cholholz Graben in clockwise direction before flowing north towards the well field located east of the Wartenberg Graben. By contrast, flow in the southwestern part is directed counterclockwise around the Hard Graben before heading Northeast towards the well field located west of the Wartenberg Graben.

Discussion

The 3D geological modeling presented in this article allowed the differences between 2D and 3D analyses of geological data to be highlighted. In order to develop a 3D geological model, data published by different authors were compiled. This model incorporated available data sets of borehole descriptions, geological cross sections and maps of varying quality and representing different interpretations by the different authors. Based on our experience, discrepancies between different data sets are difficult to reconcile using 2D data alone. The construction of the 3D geological model initiated a discussion on four fundamental discrepancies in the different geological interpretations, relating to (1) whether the area is affected by thin-skinned or thick-skinned tectonics (the depth and shape of graben structures), (2) the existence of tear faults, (3) the coherences between the Adlerhof Anticline and the Aspenrain Fault, and (4) the ending of graben structures to the south. These aspects are discussed in more detail in the sections below.

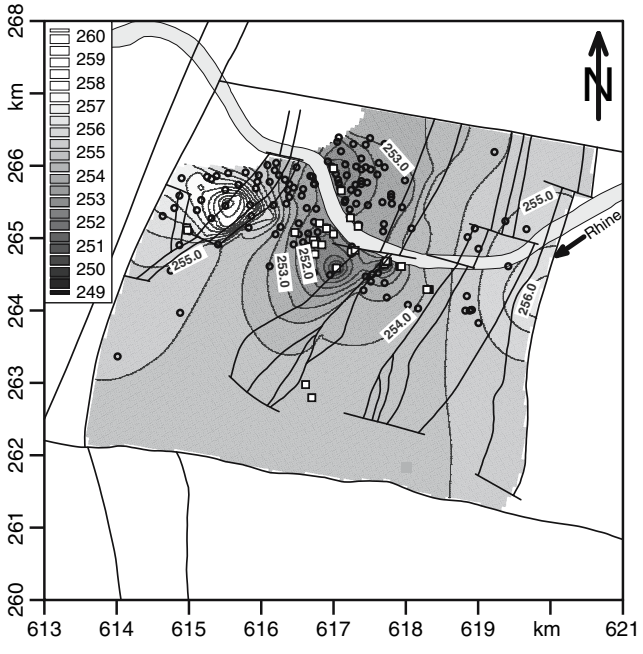

Fig. 9 Simulated piezometric head in Upper Muschelkalk aquifers is calculated with calibrated groundwater model, and corresponds to August 8th, 2003. *Black circles* are measurement locations, *black squares* are pumping wells or ponds for artificial recharge. Background shows fault system on pre-Quaternary surface

Thin-skinned or thick-skinned tectonics

If the faults of graben structures in the modeled area are considered to be listric (Herzog 1956; Schmassmann 1990), then they should end in a detachment horizon according to the theory of thin-skinned tectonics. In contrast, a straight shape of the graben structure as documented by Gürler et al. (1987) and Meyer (2001) would imply thick-skinned behavior. Our 3D geological model, which is based on well data, especially in the region of the ESE–WNW striking Adlerhof anticline, shows a planar top of the Lower Muschelkalk, but a folded top of the Sulfatzone (Fig. 7E, F). These arguments favor the thin-skinned theory. The Wartenberg-graben system shows a displacement of approximately 200 m from the eastern master fault and a displacement of about 10 m at his western master fault. Faults inside the Wartenberggraben coupled with the dip of layering indicate a stepwise rotation of graben blocks. Such rotations are typical for listric fault systems. These arguments favor listric fault shapes and a thin-skinned tectonic deformation.

On the other hand, significant evidence exists for thick-skinned tectonic activity generating the Rhine Valley Flexure, the Grenzach-Wyhlen Fault and the Aspenrain Fault. Well data and outcrop data document a displacement of 80 m on the Grenzach-Wyhlen Fault and 150 m on the Aspenrain Fault in the Lower Muschelkalk Horizon (Figs. 6A, 7F). Because these faults exist also below the Sulfatzone they were modeled with straight fault geometries.

Consequently, both thin-skinned and thick-skinned tectonic features are believed to occur in the modeled area.

Existence of tear faults

The thin-skinned NNE–SSW striking graben structures are divided into parts by W–E oriented tear faults. The interpretations of authors such as Herzog (1956) and Schmassmann (1990) show graben structures with smooth-shaped fault traces and graben systems consisting of only one part. The availability of new data suggests that this model is inadequate since faults would have to change their orientation by more than 90°. The

tear faults presented in the current model simplify the situation by a differentiation of the graben systems into parts (Fig. 5). An interesting aspect of these tear faults is the correspondence between the course of the river Rhine and their orientation.

Coherences between the Adlerhof Anticline and the Aspenrain Fault

The Adlerhof Anticline is located to the north of the Aspenrain Fault. This Fold is a thin-skinned element with a slightly dipping northern limb and a more steeply dipping southern limb (Fig. 6C). Within the anticline, south verging thrusts could be observed during the construction of the Adlertunnel (Meyer 2001). However, there is no evidence that these thrusts are connected to the Aspenrain Fault. In contrast to the Aspenrain Fault, the displacement along these south verging thrusts is relatively small. Laubscher (2003) wrote: "... the Adlerhof Fold passes into pronounced south-verging thrusts, and is accompanied in the south by a south-verging flexure." Outcrops near position 618.900/261.400 (SNTG) reveal the presence of sediments of Liassic age next to Upper Dogger with the entire Opalinuston (about 100 m) absent. This is inconsistent with Laubscher's theory of an unfaulted flexure. A fault could better explain the absence of the Opalinuston, namely due to the activity of the Aspenrain Fault. Consequently, it is necessary to incorporate (a) the thin-skinned Adlerhof Anticline, in which south-verging thrust faults are involved, and (b) the reactivated thick-skinned Palaeozoic Aspenrain Fault, south of the fold. Instead of using the simplified nomenclature "Adlerhof Structure" (Laubscher 2003) we propose the terms "Adlerhof Anticline" and "Aspenrain Fault".

Termination of graben structures to the south

An important question concerning hydraulic connections relates to the termination of graben structures to the south of the area. Schmassmann (1990), Bitterli-Brunner et al. (1984), Gürler et al. (1987), and Herzog (1956) proposed that graben structures end north of the Adlerhof Anticline. But these models cannot explain why the graben structures do not continue to the Aspenrain Fault. If extension occurred first, the graben structures would extend to the Aspenrain Fault and would be folded in a later period. On the other hand, if the folding occurred first, the Adlerhof Anticline should be affected by the extension and the development of the graben structures.

In the area of the Cholholz graben and the Adler graben, both outcrop and drill core data from the Adlertunnel railway tunnel document narrow graben structures ending to the north of the Adlerhof Fold. Furthermore, large displacements with respect to the same reference horizon between the graben interior at the southern end and the hinge line of the fold support this hypothesis (Fig. 7D, E).

In order to find a plausible explanation for this dilemma, the evolution of the regional stress field needs to be considered. A critical question is whether it is possible to form compressive structures in an extensive stress field, thereby developing the Adlerhof Fold and graben structures at approximately the same time.

Revised conceptual model

The study area is situated in the Rhine-Bresse Transfer Zone (Fig. 1). This region is characterized by strike-slip components. The Aspenrain Fault is a Palaeozoic structure, that acts as the southern boundary of the model area and part of this transfer zone. To simplify its development, Rhine Graben formation will be subdivided into two phases (Schumacher 2002). These consist of a sinistral phase operating from the Middle Eocene to Late Oligocene and a dextral phase starting in the Early Miocene. During the initial phase, the stress field orientation of the main extensional direction varied from E–W to SSE–NNW, and led to the opening of the Rhine Graben. The development of the fault system on the most southeastern Rhine Graben border was influenced by sinistral movements along the Aspenrain Fault, which led to the formation of the Bay of Dornach (Fig. 2). The detachment of the southeastern Rhine Graben border along the Aspenrain Fault is also documented by a significantly gentler dip of the border fault in the Bay of Dornach compared to fault sections north of the Aspenrain Fault. The NNE–SSW trending graben structures (inclusive tear faults) developed simultaneously, similar to the en-échelon ordered sections of the Adlerhof Anticline (strinking ESE–WNW) to the north of the Aspenrain Fault. During the second phase, which is characterized by SSE–NNW oriented compression, tear faults dextrally divided the graben structures into several sections, and south-verging thrusts developed in the core of the Adlerhof anticline. The proposed kinematical model requires a decoupling, which occurs in the 130 m thick evaporitic zone of the Middle Muschelkalk.

Consequences for groundwater flow

The geological model discussed has important consequences for the connectivity of aquifers within the hydrogeological model. The graben structures are important elements of the hydrogeological model, as the position and the dip of the formations within the graben determine the connectivity of aquifers across fault zones. If the graben structures continue up to the Aspenrain Fault, and hence cut through the Adlerhof Anticline, then the groundwater connectivity within the Upper Muschelkalk Aquifer would not be possible between horsts. However, in the present hydrogeological model, groundwater flow is not restricted to the southern border of the

model. In fact, the productivity of the large-scale industrial pumping in the central part of the model area can only be supported with groundwater recharge from adjacent horsts. Since groundwater flow across graben structures is restricted, the flow pattern within the southern part of the Upper Muschelkalk Aquifer is circular around the southern ending of the graben structures (Fig. 9).

Conclusion

This article has presented a 3D geological model incorporating thick-skinned tectonic elements such as the Rhine Valley Flexure, the Grenzach-Wyhlen Fault, and the Aspenrain Fault. Incorporated thin-skinned tectonic elements include graben structures and Adlerhof Anticline. We propose a subdivision of the graben structures by W–E striking tear faults and the termination of these graben structures to the north to the Adlerhof Fold. This anticline consists of a number of ESE–WNW striking parts arranged in an en-échelon configuration. The Aspenrain Fault to the south of the anticline is a reactivated Paleozoic feature. No evidence can be found for a combined "Adlerhof Structure" as presented by Laubscher (2003) using the current approach. Consequently, the names "Adlerhof Anticline" and "Aspenrain Fault" are proposed and should be considered as separate structures.

The development of the modeled structures consists of two steps:

- Simultaneous development of NNE–SSW trending graben structures (inclusive tear faults) and en-échelon ordered Adlerhof Anticline parts (ESE–WNW striking) during an extensional stress-field, E–W to SSE–NNW trending, and lasting from the Middle Eocene to the Late Oligocene.
- Subdivision of graben structures by tear faults under dextral movements in a SSE–NNW oriented compressive stress field, starting in the Early Miocene.

The geological model itself consists of 47 faults, including the Rhine Valley Flexure, the Grenzach-Wyhlen Fault, the Aspenrain Fault and four narrow graben systems (Hard Graben, Wartenberg Graben, Cholholz Graben, Adler Graben) (Fig. 5). Six stratigraphic horizons relevant for groundwater flow have been modeled, i.e. topography, pre-Quaternary surface, Top Keuper, Top Upper Muschelkalk, Top Sulfatzone and Top Lower Muschelkalk (Fig. 7).

The model provides an important database that can be used for 3D queries. Predictions about the geology of specific areas of interest can be provided with help of 2D cross-section or 1D well logs at arbitrary locations. The advantage of these predictions is that they show faults and horizons, which were constructed with a 3D interpolation algorithm. The interpolation algorithm has been constrained by geological boundary conditions, which are founded on different types of data. The presented 3D model has already been tested using more recent data, with predictions of deeper boreholes drilled for the evaluation of contaminated sites in the Muttenz area (western part of the model). The predictions were in good agreement with the collected borehole data, and confirmed the relevance of the 3D model.

The 3D numerical simulation of groundwater flow required an appropriate transformation of the 3D faults and horizons into discrete elements with distributed hydrogeological properties. We used a 3-layer approach with a horizontal regularly spaced grid combined with an irregular transmissivity distribution with depth. The simulated piezometric head of the steady-state model was automatically calibrated to corresponding measurements using more than 200 piezometers. Model results demonstrated the effect of the large-scale industrial pumping in the central part of the model (up to 1500 l/s), where the groundwater flow field in the Upper Muschelkalk aquifer is affected at distances of up to 2 km to the south. The productivity of these wells can only be supported by groundwater recharge from adjacent horsts inducing a circular flow pattern around the southern end of the graben structures (Fig. 9).

The results presented provide the basis for further modeling of salt dissolution and solute transport. They will help to focus on the causes and mechanisms of the salt solution phenomena in Mid-Triassic evaporites, and may ultimately help control widespread land subsidence risks in the study area.

Acknowledgements We would like to thank the "Amt für Umweltschutz und Energie Basel Landschaft" for funding this project. Many thanks to Kamil Ustaszewski for discussing the regional geology, especially the Adlerhof Anticline–Aspenrain Fault situation. We would also like to thank Karin Bernet, Ray Flynn, Martin Mazurek and David Tanner for their valuable reviews of the manuscript and Ralph Kirchhofer for his technical support during the project.

References

Aegerter I, Bosshardt AG (1999) Technischer Bericht–Setzungsproblematik/Massnahmen gegen die Setzungen

Bitterli-Brunner P, Fischer H (1989) Erläuterungen zum Blatt Arlesheim 1067. Geologischer Atlas der Schweiz

Bitterli-Brunner P, Fischer H, Herzog P (1984) Geologische Karte Blatt Arlesheim 1067. Geologischer Atlas der Schweiz

D'Agnese FA, Faunt CC, Hill MC, Turner AK (1999) Death Valley regional ground-water model calibration using optimal parameter estimation methods and geoscientific information systems. Adv Water Resour 22(8):777–790

GMS (2004) Groundwater modeling system v4.0. Environmental Modeling Systems, Inc., South Jordan (Utah), USA

Gürler B, Hauber L, Schwander M (1987) Die Geologie der Umgebung von Basel mit Hinweisen über die Nutzungsmöglichkeiten der Erdwärme. Beitrag zur Geologischen Karte der Schweiz

Harbaugh AW, Banta ER, Hill MC, McDonald MG (2000) MODFLOW-2000, The U.S. geological survey modular ground-water model-user guide to modularization concepts and the ground-water flow process. US Geological Survey Open-File Report 00–92

Hauber L (1971) Zur Geologie des Salzfeldes von Schweizerhalle-Zinggibrunn (Kt. Baselland). Eclogae geol Helv 64(1):163–183

Herzog P (1956) Die Tektonik des Tafeljura und der Rheintalflexur südöstlich von Basel. Eclogae geol Helv 49(2):317–362
Jussel P, Stauffer, F, Dracos T (1994) Transportmodeling in heterogeneous aquifers: 1. statistical description and numerical generation of gravel deposits. Water Resourc Res 30(6):1803–1817
Kovacs A (2003) Geometry and hydraulic parameters of karst aquifers: A hydrodynamic modeling approach.; Thèse de Doctorat, CHYN, Univ de Neuchâtel
Laubscher H (1971) Das Problem von Rheintalflexur und Tafeljura. Eclogae geol Helv 64(1):157–162
Laubscher H (1982) Die Südostecke des Rheingrabens–ein kinematisches und dynamisches Problem. Eclogae geol Helv 75(1):101–116
Laubscher H (2001) Plate interactions at the southern end of the Rhine graben. Tectonophysics 343:1–19
Laubscher H (2003) The Miocene Dislocations in the northern foreland of the alps: oblique subduction and its consequences (Basel area, Switzerland-Germany). Jber Mitt Oberrhein geol Ver 85:423–439
Mallet JL (1989) Discrete smooth interpolation. ACM Trans Graph 8(2):121–144
Mallet JL (1992) Discrete smooth interpolation in geometric modeling. CAD 24(4):178–191
Mallet JL (2002) Geomodeling. Oxford University Press, pp 1–600
Meyer M (2001) Die Geologie des Adlertunnels. Bull Angew Geol 6(2):199–208
Nagra (1988) Sedimentstudie– Zwischenbericht 1988. NTB:88–25
Nagra (2002) Projekt Opalinuston: Synthese der geowissenschaftlichen Untersuchungsergebnisse. NTB:02–03
Noack T (1993) Geologische Datenbank der Region Basel. Eclogae geol Helv 86(1):283–301
Pearson FJ, Balderer W, Loosli HH, Lehmann BE, Matter A, Peters T, Schmassmann H, Gautschi A (1991) Applied Isotope Hydrogeology—a case study in northern Switzerland. Elsevier
Poeter EP, Hill MC (1998) Documentation of UCODE, a computer code for universal inverse modeling. USGS WRIR 98–4080, pp 1–116
Regli C, Rosenthaler L, Huggenberger P (2004) GEOSSAV: a simulation tool for subsurface applications. Comput Geosci 30:221–238
Schmassmann H (1990) Hydrogeologische Synthese des Rheintals zwischen Ergolz und Birs. Bericht des Amtes für Umweltschutz und Energie Basel- Landschaft
Schumacher M (2002) Upper Rhine Graben: role of preexisting structures during rift evolution. Tectonics 21(1)
Thury M, Gautschi A, Mazurek M, Müller WH, Naef H, Pearson FJ, Vomvoris S, Wilson W (1994) Geology and hydrogeology of the crystalline basement of northern Switzerland—synthesis of regional investigations 1981–1993 within the Nagra Radioactive Waste Disposal Programme. Technical Report 93–01
Trösch J, Kuhlmann U, Junghans U, Noack T (1997) Grundwassermodell Hardwald–Modellaufbau und Kalibrierung. TK Consult AG and Geologisch-Päontologisches Institut der Universität Basel, Bericht des Amtes für Umweltschutz und Energie Basel-Landschaft
Wittmann O, Hauber L, Fischer H, Rieser A, Staehelin P (1970) Geologische Karte Blatt Basel 1047. Geologischer Atlas der Schweiz
Zechner E, Frielinsdorf W (2004) Evaluating the use of data on canal seepage and solute concentration in aquifer parameter estimation. J Hydrol 289:62–77